

## WEATHERING OF BIOTITE: MICRO TO NANO SCALE REACTIONS IN THE REGOLITH

Mehrooz F Aspandiar<sup>1</sup> and Tony Eggleton<sup>2</sup>

<sup>1</sup>Department of Applied Geology, CRC LEME, WASM, Curtin University of Technology

<sup>2</sup>Department of Earth and Marine Sciences, CRC LEME, Australian National University

### INTRODUCTION

The chemical and physical weathering of minerals is the fundamental process giving rise to much of the regolith and affects critical processes of the regolith such as metal release and retardation (dissolution-precipitation) and adsorption. Although our understanding of mineral weathering reactions for most primary minerals is extensive from a unit cell scale (Hochella & Banfield 1995), knowledge of micro environments on mineral weathering remains limited. The processes and products of weathering of biotite has been extensively studied both in the laboratory and in under natural conditions with the type of end products considered to be dictated by the conditions experienced by the soil such as acidic, leached or waterlogged (Wilson 2004). The main mechanism is considered to be the oxidation of Fe<sup>2+</sup> in the mica with subsequent release of K from the interlayers to form “hydrobiotite” and subsequently vermiculite, which involves only a structural adjustment. Further release of K as solution access increases results in the formation of kaolinite and goethite, with studies finding different alteration products such kaolinite or halloysite and goethite. However, the biotite weathering investigations do not consider the weathering products on microsites within individual biotite grains, and each biotite grain and the regolith unit in which it is weathering potentially has a story to tell on weathering reactions and products. The aim of this article is to investigate the different mechanisms and products that arise in different microsites within a weathering profile evolved on a granodiorite.

### SAMPLES AND METHODS

A weathering profile evolved over a granodiorite and underlying an erosional rise was sampled. The sampling location is within the Ravenswood Batholith, 20 km SW of Charters Towers, Queensland. The fresh granodiorite, saprock, saprolite, upper saprolite and soil horizon samples were dried, impregnated with resin under vacuum and subsequently sectioned to approximately 30 µm. Optical and backscattered electron (BSE) imaging was conducted on the thin sections to observe microscopic reactions of individual biotite grains. The areas showing different weathering products were then selected for Transmission Electron Microscopy (TEM) including analytical electron microscopy (AEM) by placing Cu grids and ion beam thinning to make it electron beam transparent. During ion thinning, care was taken to thin microsites identified via BSE.

### RESULTS

#### Optical/BSE

In the saprolite, nearly half the biotite grain(s) were pseudomorphed by secondary products which show loss of colour and pleochroism of the original mica (Bt-V in Figure 1A). In addition to such pseudomorphs which preserve the cleavage habit of the original biotite, regions 1-5 µm wide and 10-100 µm long and having a brown dark grey colour and granular texture, appear to be iron rich in BSE image (F in Figure 1A). In addition to these alteration signs observed in the saprolite, the biotite grains in the upper saprolite are broken up via fissures which bear argillans (Ar in Figure 1A). The argillans appear to push apart the biotite layers and enter into the original grain possibly along cleavages. Therefore, in the upper saprolite, three distinct sites of biotite weathering can be observed: pseudomorphic replacement within the grain, granular textured material within zones along cleavages and destruction of original biotite grain along fissures manifested by argillans (Figure 1A). All these sites were studied for reactions products via TEM.

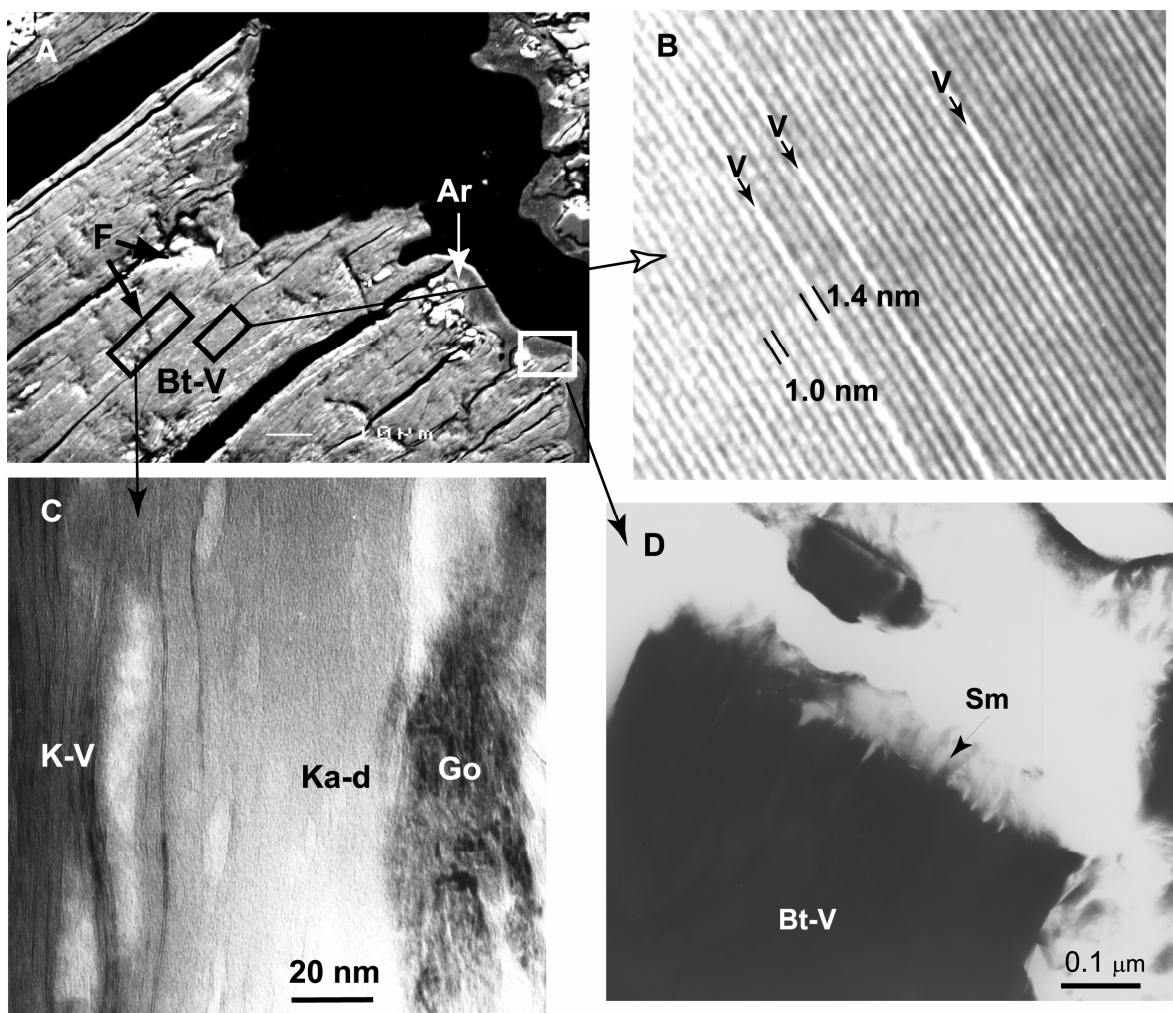


**Figure 1.** Mosaic of biotite weathering products in different microsites. **A.** A backscattered electron image (BSE) of biotite grain from the upper saprolite, showing weathering products pseudomorphing biotite (Bt-V), high atomic contrast products along cleavage planes (F) and argillans (Ar) invading weathered biotite grain. **B.** A HREM image of Bt-V area in (A), showing 1.0 nm mica layers interstratified with 1.4 nm vermiculite layers (V). **C.** Area marked F from (A) showing gradation from 0.7 and 1.4 nm layers (K-V) to damaged kaolinite (Ka-d), to small grains of goethite (Go). **D.** TEM image of contact between argillans and weathered biotite in (A) showing weathering products after biotite (Bt-V) altering to smectite (Sm).

### TEM

Observations in the area pseudomorphing biotite indicates presence of packets of phyllosilicates (Figure 1B). The dominant layers show a 1.0 nm repeat, which together with selected area electron diffraction (SAED) patterns was interpreted as biotite. Among these 1 nm layer fringes, lighter regions are present, the spacing of which varies from 1.2-1.4 nm (V in Figure 1B). These regions commence within the biotite layers. These wider layers do not show a regular pattern of alternating 1.0 nm and 1.4 nm, but are random. Selected area electron diffraction (SAED) patterns of the region show streaking along the [00l] of the biotite, which indicates the presence of another interlayered phase. The wider layers are interpreted as vermiculite and develop within biotite packets. The reaction of one biotite to one vermiculite layer is thus clear from the TEM lattice fringe image, a fact previously documented by Banfield and Eggleton (1988). No extensive alteration of biotite to vermiculite and no regular interstratification of the two was noticed in accordance with the above workers.

In the saprolite samples, TEM observations displayed smaller packets or zones 5-10 nm in thickness and parallel to (001) direction of biotite-vermiculite packets, but damaged rapidly on exposure to the electron beam. In some places, an assemblage of 1.0 nm and 0.7 nm layer repeats were seen (Figure 1C). Diffraction patterns of these packets show layer spacings of 1.0, 0.8-0.9 and 7 nm, with their (00l) and (010) to be parallel (SAED data). The 0.7 nm layer spacing is interpreted to be kaolinite and the 0.8-0.9 nm spacing is interpreted as biotite-kaolinite interstratification, and the variable spacing indicates a dominant random interstratification, although regularity could be possible within some packets. Alteration to kaolinite was always seen to commence within zones and move across the (001) direction of biotite packets, rather than showing regular interstratification throughout the biotite layers. No direct observation of biotite-vermiculite to kaolinite layer was observed as documented by Dong *et al.* (1998).

Observations in the reddish granular textured material displayed packets of biotite-vermiculite layers with narrow zones of damaged material adjoining 0.2-0.5  $\mu\text{m}$  zones of damaged material, which further grades into a granular textured material (Figure 1C). The analysis of the damaged material showed mainly Al-Si and a few 1.0 nm layers were present in the damaged material. On the basis of rapid damage and chemistry, the damaged material is interpreted as kaolinite with a few interstratified vermiculite layers. The granular textured material adjoining the damaged material was identified as goethite via its micro-diffraction pattern. The entire sequence showing in Figure 1C is interpreted as biotite-vermiculite altering to kaolinite and goethite. No biotite layers were observed in direct contact with goethite.

Observations along the boundary of the biotite and argillan (Figure 1A) show coarse packets of biotite-vermiculite altering to flaky phyllosilicate packets (Figure 1D). Due to textural differences between materials, ion beam thinning was uneven and hence high resolution imaging of the contact between the flaky packets and biotite were difficult to obtain. Diffraction patterns showed variable d-spacings between 1.0-1.3 nm along the (001) of the phyllosilicates, and its chemistry as determined by AEM was dominated by Al, Si and to a lesser extent Ca and Mg. On this basis the flaky phyllosilicates is interpreted as a collapsed 2:1 phyllosilicate, ideally smectite, although there could possibly be interlayers of mica or kaolin.

## DISCUSSION AND CONCLUSIONS

The above observations indicate the existence of several biotite weathering products in varying amounts at different sites within one single grain aggregate of biotite and is likely due to the hydrodynamics of the microsites (Hochella & Banfield 1995). The first microsite evolves away from microscopically observable solution passages such as fissures and cleavages, and is dominated by a structurally coherent 2:1 random interlayered phyllosilicate - biotite-vermiculite (B-V). Kaolinite packets are present within these B-V packets and the common orientation of the axes of these layer silicates is indicative of strong growth control, although to form kaolinite from vermiculite some partial dissolution of vermiculite is necessary (Banfield & Eggleton 1988) rather than pure topotactic reaction. The second microsite is dominated by granular textured material made up of goethite crystal aggregates surrounded dominantly by kaolinite and kaolinite-vermiculite forming along cleavages. The added solution access provided by cleavages favours a faster reaction of vermiculite to kaolinite with the released Fe migrating to nano-pores present along grain boundaries and crystallizing as goethite. The third microsite is adjoining the argillans present in the fissure where biotite (or biotite-vermiculite) alters to a flaky smectite which may posses some interlayering of a mica-kaolin. The last type of microsite allows much greater access of solutions and thereby reaction rates are faster with the chemistry of the solution affecting the chemistry of the secondary products (smectite). The documentation of different reaction products having variable structural and chemical control from the host biotite, having evolved in different microsites demonstrates that weathering reactions are complex and the products developed diverse, even within a single parent mineral grain, let alone the profile.

**REFERENCES**

- BANFIELD J.F. & EGGLETON R.A. 1988. TEM study of biotite weathering. *Clays and Clay Minerals* 36, 47-60.
- DONG H., PEACOR D.R. & MURPHY S. 1998. TEM study of progressive alteration of igneous biotite to kaolinite throughout a weathered soil profile. *Geochemica Cosmochimica Acta* 62, 1881-1887.
- HOCELLA M.F. & BANFIELD J.F. 1995. Chemical weathering of silicates in nature: A microscopic perspective with theoretical considerations In: WHITE A.F. & BRANTLEY S.L. (ed), *Chemical weathering rates of silicate minerals*, 31. Mineralogical Society of America, Washington DC, 353-406.
- WILSON M.J. 2004. Weathering of the primary rock-forming minerals: processes, products and rates. *Clay Minerals* 39, 233-266.